JOURNAL OF MATERIALS SCIENCE 28 (1993) 1843–1848

Influence of the phase compositions on the transient-stage high-temperature oxidation behaviour of an NiCoCrAlY coating material

S. SACRÉ, U. WIENSTROTH, H.-G. FELLER, L. K. THOMAS
Institut für Metallforschung der TU Berlin, Berlin, Germany

The oxidation behaviour of a commercial NiCoCrAlY coating material (H. C. Starck Inc.; Amperit 410) was investigated in the temperature range 850–1200 °C. The measurements were made in air under isothermal and cyclic conditions. The oxidation process was quantified by thermogravimetry. The oxide compositions were characterized by energy-dispersive X-ray analysis (EDX), X-ray diffraction (XRD), X-ray photoelectron spectroscopy (XPS) and secondary-ion mass spectroscopy (SIMS). The corresponding oxide morphologies were studied by scanning electron microscopy (SEM). This study was focused on the oxide growth of a NiCoCrAlY alloy at temperatures between 850 and 1200 °C up to oxidation periods of 25 h. Complementary information obtained from various surface-sensitive techniques are summarized in a simplified scheme of the oxide growth. The oxidation behaviour in the stated temperature range is explained by the different chromium and aluminium contents of the phases. Yttrium becomes effective at temperatures above 1000 °C. The good protective properties of the NiCoCrAlY at temperatures above 1000 °C and the fairly poor protection below 950 °C are interpreted in terms of alumina formation and chromia formation as rate-determining factors.

1. Introduction

One of the fundamental problems in materials engineering is to find materials with outstanding properties with respect to the specific application. However, it is not always possible to satisfy these requirements with a single material; a combination of several materials promises to combine the individual positive properties within one component. A typical example of great industrial interest is given by the high-temperature alloys used in gas turbines. The turbine blades, for example, have to withstand both mechanical and chemical loadings. Therefore, the blade is (usually) made of an Ni-base superalloy with outstanding properties with regard to creep, low cycle fatigue (LCF), etc. Unfortunately, these alloys do not resist the chemical attack resulting from oxidizing atmospheres at high temperatures. In order to use these alloys, their surfaces have to be protected by coating materials.

The development of coating materials is concentrated on alloys that form protective alumina or chromia scales. At temperatures above 1000 °C the protective properties of alumina-forming coatings are generally considered to be better than those of chromia formers [1]. This observation can be explained by the fact that chromia begins to decompose above 1000 °C, forming the volatile CrO_3. At about 850 °C the chromia-forming alloys are found to be more protective [2]. Especially in corrosive environments, the superior properties are well known [3, 4]. Depending on the specific application, the coating materials are designed for use either above 1000 °C or below 900 °C. It seems difficult to cover the entire temperature range with only one alloy.

Minor additions of rare-earth elements such as yttrium or cerium have been found to improve the protective properties of both alumina- and chromia-forming alloys [5, 6]. Although that positive effect of the rare-earth elements has been known for more than 50 years, the mechanisms involved are the subject of several investigations [7, 8].

Due to advanced spraying technologies, the development of new overlay coatings became possible [9]; the present research is concentrated on the optimization of MCrAlY (M = Co or Ni) alloys [6, 10]. In general, the composition of the oxides on MCrAlY alloys is complicated and depends on several parameters such as the temperature, oxidation time, microstructure and surface roughness. This list may easily be extended by several other parameters.

2. Experimental

Samples were prepared from commercial NiCoCrAlY alloy (H. C. Starck; Amperit 410) with the nominal composition shown in Table I. The alloy was supplied as sprayed powder which is fabricated for low-pressure plasma spraying processes. Each powder particle contained the given composition. From the powder (average grain size approximately 90 μm) compact ingots were melted in an electron-beam furnace and

0022–2461

TABLE I Nominal composition of Amperit 410

	Ni	Co	Cr	Al	Y
wt%	47.1	23.0	17.0	12.5	0.45
at%	40.3	19.6	16.5	23.3	0.26

subsequently cut into thin discs (diameter 25 mm) in order to achieve a large surface/volume ratio. EDX of the composition of the samples resulted in good agreement with the nominal composition. The slices were ground with waterproof SiC paper up to a mesh size of 1000 and subsequently ultrasonically cleaned.

Thermogravimetric measurements took place in a conventional chamber furnace in air. The oxidation periods ranged from 25 to 1000 h. The weight gain was determined after the samples were cooled. The cyclic oxidation experiments were carried out with cycle periods of 1 h. After every hour the samples were cooled on a water-cooled copper plate. It took < 2 min for the samples to reach room temperature. The total number of cycles was about 100.

The data for the thermogravimetric experiments were obtained by averaging the weight gain over several samples. The data given in Figs 2 and 11 represent mean values and the scatter of the data was usually < 0.02 mg cm^{-2}.

The oxide morphology and oxide composition were determined by SEM (Jeol 6400) with integrated EDX (Link Analytical QX200). The compounds of the oxides were identified by XRD. The diffractometer (Philips) was assisted by a computer-based American Society for Testing and Materials (ASTM) database. The compositions of the surface layers of the oxides were analysed by XPS (Leybold) and SIMS (Atomica).

3. Results and discussion

3.1. Microstructure of the alloy

The microstructure of the NiCoCrAlY showed a dendritic solidification (Fig. 1) and three phases with the compositions given in Table II. The lighter matrix was identified by XRD as Ni γ-phase whereas the dark, dendritic phase consisted of β-NiAl.

Yttrium was concentrated in a third phase in amounts up to 15 at %. The volume fraction of this phase was 1–2%, the dimension was approximately 10 μm and was localized at the grain boundaries. From the literature it is known that yttrium is bound as intermetallic M_5Y or M_3Y (M = Ni or Co) [11]. However, our measurements clearly suggested the formation of intermetallic yttride M_5Y.

3.2. Isothermal oxidation

Generally, oxidation processes are quantified by thermogravimetry. The weight gain due to isothermal oxidation is presented as a function of the oxidation time in Fig. 2. Curves are shown for samples oxidized at 850, 1000 and 1100 °C for 100 h and 1200 °C for 25 h. For the temperatures 850, 1000 and 1100 °C the weight gain increased to values of between 0.5 and 0.8 mg cm^{-2} after 25 h. At 1200 °C the oxidation process was much faster. For oxidation times < 20 h the NiCoCrAlY alloy oxidized at 1000 °C more quickly than at 1100 °C. This point is addressed in the following discussion.

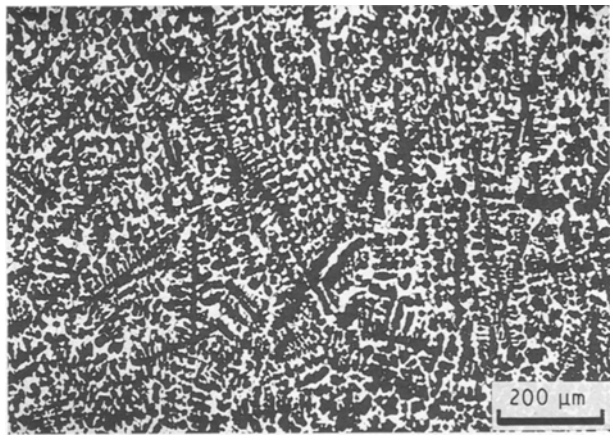

Figure 1 Phase distribution of Amperit 410.

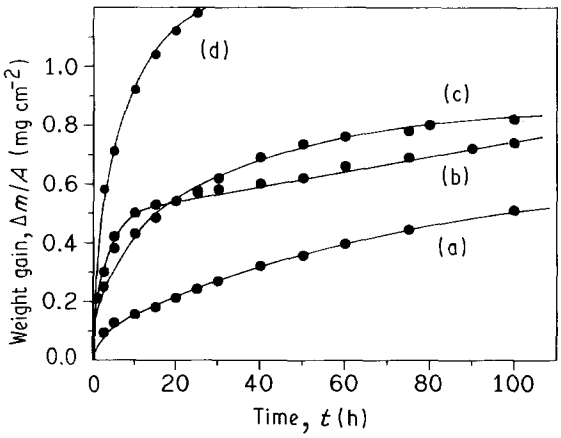

Figure 2 Isothermal oxidation at (a) 850, (b) 1000, (c) 1100 and (d) 1200 °C.

TABLE II Phase compositions (in at %)

Phase	Ni	Co	Cr	Al	Y
Ni γ-phase	35.8	28.4	26.4	9.4	
(NiAl) β-phase	43.9	18.1	11.1	26.9	
$(NiCo)_5Y$	52.1	16.1	6.5	11.1	14.2

The measured curves are interpreted in terms of the parabolic rate constant k_p. This constant is defined by the equation $(\Delta m/A)^2 = k_p t$, where $\Delta m/A$ denotes the weight gain per unit surface area and t is the oxidation period.

It must be mentioned that the relationship between weight gain and oxidation time is not exactly parabolic, so the calculated constants should be called "pseudo-parabolic". Despite this restriction, the calculation of k_p is instructive in comparing the oxidation rates of different alloys.

The calculated values of k_p are shown in Fig. 3 as an Arrhenius plot as a function of the oxidation temperature, together with data given by Lillerud and

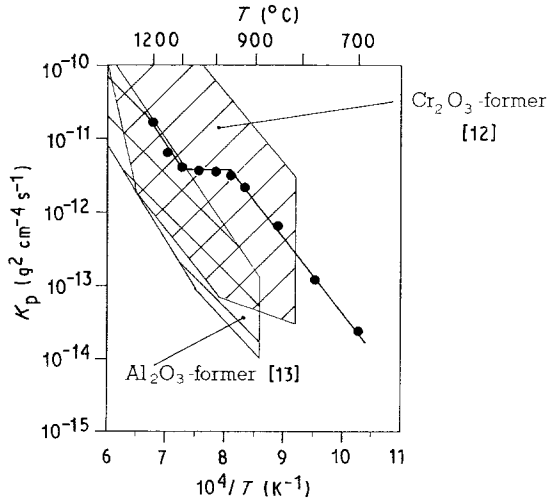

Figure 3 Arrhenius plot of k_p versus oxidation temperature.

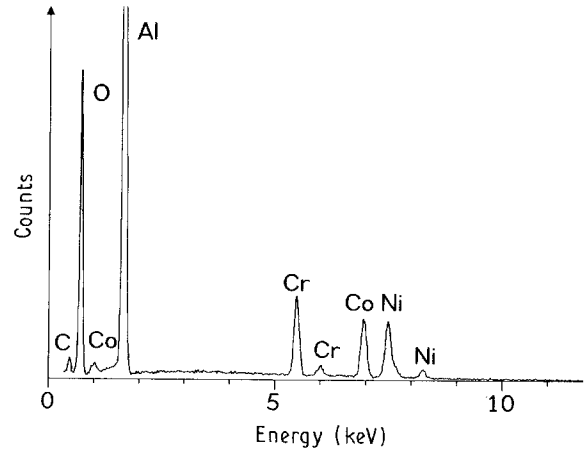

Figure 4 EDX spectrum of a sample oxidized for 25 h at 850 °C: (at %) Co 0.4, Cr 0.6, Al 38.8 and O 59.8.

Kofstadt [12] and Hindam and Whittle [13]. The Arrhenius plot shows three regions of interest.

3.2.1. Range I: $T < 1000$ °C

In the temperature range from 700 °C to approximately 1000 °C a linear relationship between log k_p and $1/T$ exists. The results of Lillerud and Kofstadt [12] suggest chromia formation. However, EDX analysis identified the oxides that were oxidized for 25 h as alumina with small amounts of chromia, nickel and cobalt oxide (Fig. 4); yttrium was not found.

XPS analysis of the outer layer of the oxide suggested the formation of pure alumina; chromia, cobalt or nickel oxide not being found. In addition, no yttrium or yttrium compounds were formed (Fig. 5a–d). It is conspicuous that the XPS spectra of the oxides are shifted to high binding energies compared with the literature values [14]. This phenomenon is explained by the formation of a thin alumina scale with a low electrical conductivity. This leads to a charging of the sample and therefore shifted electron energies were measured.

SIMS measurements confirmed both the EDX and XPS results. Due to an insulating oxide film (alumina), the detection of the secondary ions was not possible for the first 250 nm of the oxide (Fig. 6). At greater depths an analysis of the oxide composition became possible. In the surface region decrease in the concentration of the elements Cr, Ni (Co) and Y was found.

Since the information depth of XPS reaches only roughly 2 nm, the outer alumina scale was confirmed by SIMS. In contrast, the information depth of EDX analysis reaches several μm, and therefore the other elements (Cr, Ni and Co) were detected.

The investigations at 850 °C were supplemented by XRD measurements of samples that were oxidized for 1000 h. Under these conditions the formation of both alumina and chromia was observed. The alumina scale was disconnected by chromia crystallites which were randomly distributed (Fig. 7a and b). The growth of these crystallites was very regular and the surfaces smooth.

The results obtained at 850 °C can be summarized and interpreted on the basis of a simplified model. The unoxidized alloy consists of γ-Ni and β-(NiAl) phases which are separated by an M_5Y phase (Fig. 8, t_0). The first stage of the oxide growth is assumed to be governed by alumina formation (t_1). This view is supported by the very low value of ΔG for the formation of alumina. The formation of that alumina scale leads to a decrease in the aluminium content in the alloy beneath the oxide. If the decrease in the aluminium content in the γ-Ni phase reaches a critical value, the content of aluminium is no longer sufficient to form a protective alumina scale and internal oxidation of chromium begins. Since yttrium is bound in a stable intermetallic phase, it does not influence the oxide growth. While the alumina formation on the β-(NiAl) phase continues, mechanical stresses between the internal oxides and oxide scales at the surface on the γ-Ni phase lead to cracks in the brittle outer alumina scale (t_2). These cracks cause an outwards growth of chromia (t_3). A lateral growth of chromia on the surface may be possible.

According to this model the oxidation rate is determined by the formation of chromia. This reasoning is supported by the values of the parabolic rate constant k_p which are typical for chromia-forming alloys (Fig. 3).

3.2.2. Range II: 1000 °C < T < 1100 °C

This temperature range cannot be described by a single oxidation mechanism. Both chromia and alumina formation are superimposed. With increasing temperature the dissolution of the intermetallic M_5Y phase proceeds and therefore causes alumina formation (see also range III, below).

This view is supported by the Arrhenius plot, which shows rate constants k_p almost independent of the oxidation temperature (Fig. 3). Since this behaviour cannot be understood as a single thermally activated process, an interpretation by a transition seems reasonable. Further experimental evidence is given by EDX, XPS and SIMS analysis. With increasing temperature the concentration of aluminium (bound as alumina) on the surface decreases continuously (XPS, Fig. 5) and the amount of alumina in the oxide increases (EDX). However, the observed changes in the oxide composition are only minor.

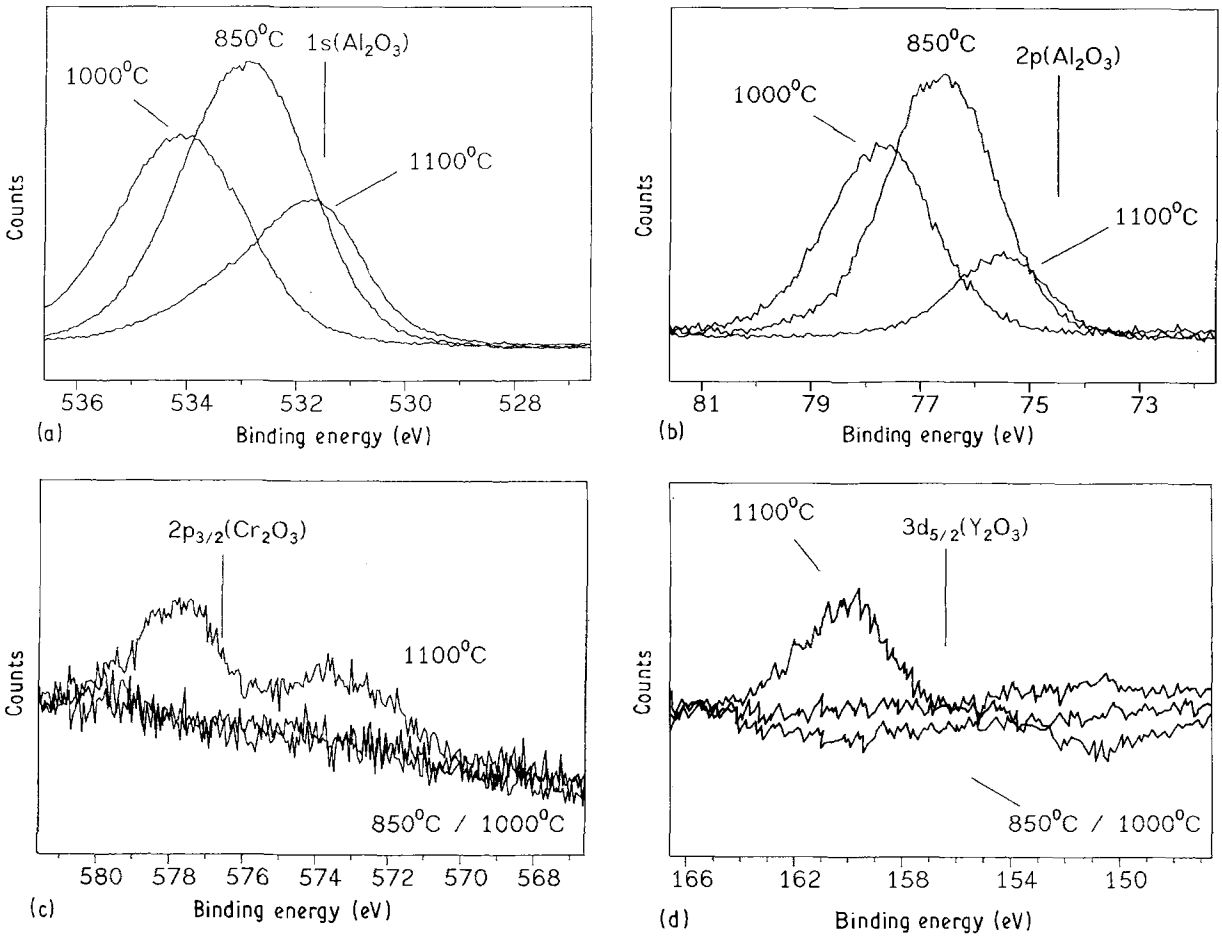

Figure 5 XPS spectra of samples oxidized for 25 h for the elements (a) O, (b) Al, (c) Cr and (d) Y.

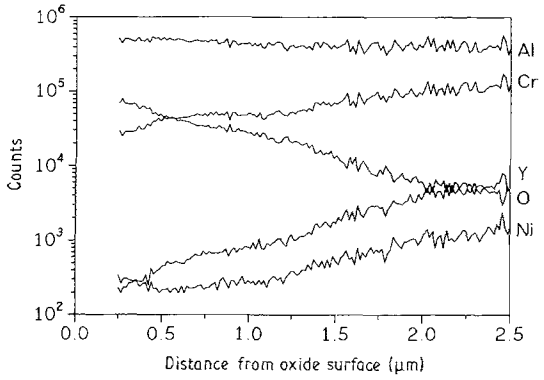

Figure 6 SIMS depth profile of a sample oxidized for 25 h at 850 °C.

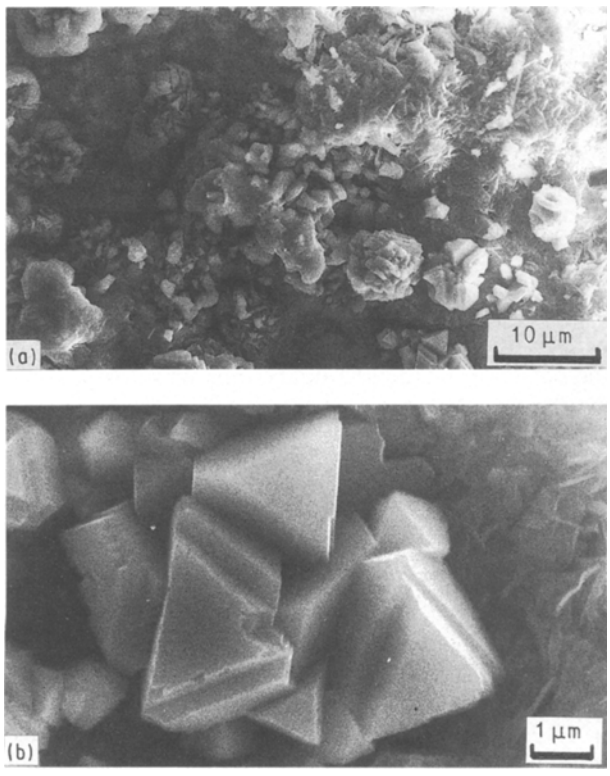

Figure 7 Oxide morphology of a sample oxidized at 850 °C for 1000 h.

The transition can be characterized best by the changes in the oxide morphology. At 1000°C the oxide consists of sharp needles, the structure being loose (Fig. 9a). With increasing temperature the sharp needles disappear and the oxide becomes more compact (Fig. 9b and c) [15].

3.2.3. Range III: $T \geq 1100$ °C

The positive yttrium effect does not become completely effective until the oxidation temperature exceeds 1100° The values of k_p are in accordance with data for chromia [12] and alumina [13]. At 1100 °C the oxide scale consists mainly of alumina (by EDX), the amount of chromia, cobalt and nickel oxide is reduced compared with oxides formed at 850 °C. The phases Al_2O_3, Y_2O_3 and $Y_3Al_5O_{12}$ (YAG) were identified by XRD. Contrary to the results obtained at lower temperatures, several oxides (alumina, chromia, cobalt and nickel oxide) were detected in the outer

subscale by XPS (Fig. 5). SIMS analysis confirmed considerable amounts of yttrium and aluminium in the oxide scale.

The kinetics of the oxide growth can be illustrated by simple model. Since the M_5Y phase dissolves at temperatures higher than 1000 ° C, the selective oxidation of Cr(Co,Ni) is improved [16]. Therefore, γ-Ni phase forms in addition to Al_2O_3 major amounts of Cr_2O_3, NiO and CoO, whereas the β-(NiAl) phase forms solely alumina (Fig. 10, t_1). Due to the different growth mechanisms of alumina (inwards) and chromia (outwards) [1], further growth of the outer chromia scale is suppressed by a separating alumina scale (t_2). While the growth of the alumina scale (together with yttria) continues, chromia decomposes and evaporates as CrO_3. The remaining oxides of cobalt and nickel transform to (Co, Ni) Al_2O_4. The reaction of Y_2O_3 and Al_2O_3 to YAG leads to precipitations of YAG at the boundary of the oxide and alloy (t_3). This reasoning suggests the growth of alumina as the rate-determining factor.

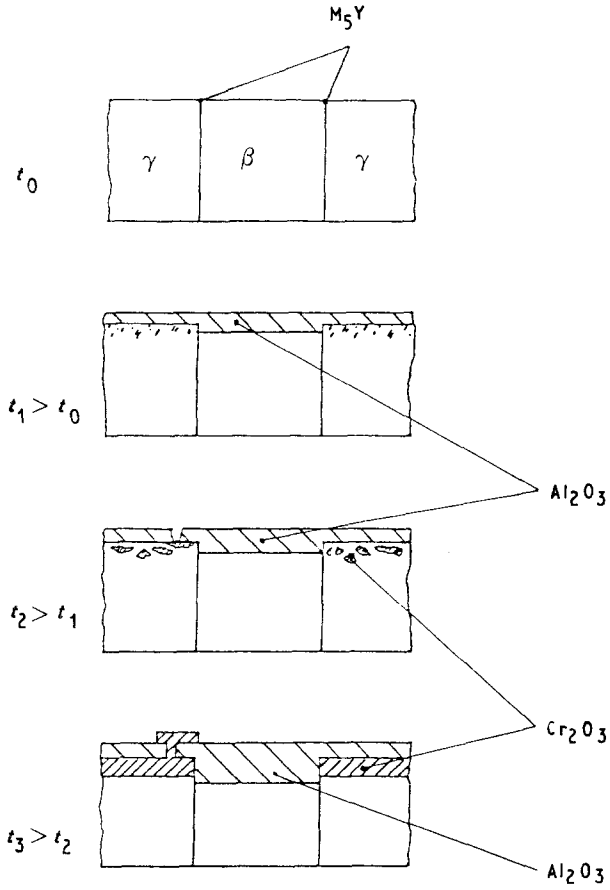

Figure 8 Model of the oxidation mechanism at 850 °C.

At about 1200 °C a spalling of the oxide is observed if the sample is cooled to room temperature. The spalled oxide consists of YAG and Al_2O_3, no Y_2O_3 being found. The adherence of the oxide seems to be guaranteed as long as yttrium is bound as Y_2O_3. The adherence is reduced if the solid-state reaction of Y_2O_3 to YAG is completed. This idea is supported by the literature, which reports the positive effect of Y_2O_3 with regard to scale adherence due to "pegging" [7, 17].

3.3. Cyclic oxidation

At temperatures of 1000 and 1100 °C the oxidation rates obtained under cyclic conditions were comparable with the results for the isothermal experiments (Fig. 11); no differences were found up to 300 cycles (300 h) at 1000 °C or 100 cycles (100 h) at 1100 °C. This proves the outstanding thermal shock resistance of the alloy.

At 1200 °C the coating material broke down. Due to spalling of the oxide, a loss of weight was observed. The spalled oxide had the same composition (Al_2O_3 and YAG) as the oxides investigated after isothermal oxidation.

4. Conclusions

1. At temperatures below 1000 °C the oxidation rate was determined by chromia formation. Yttrium was

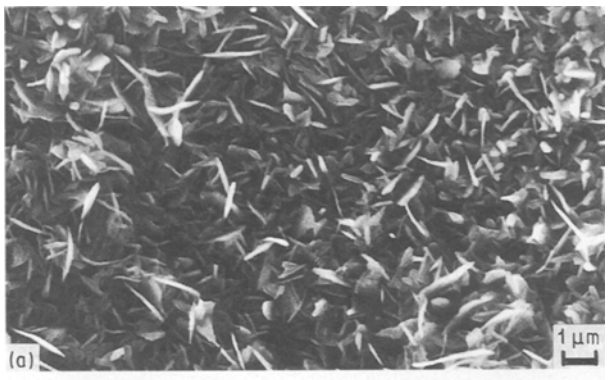

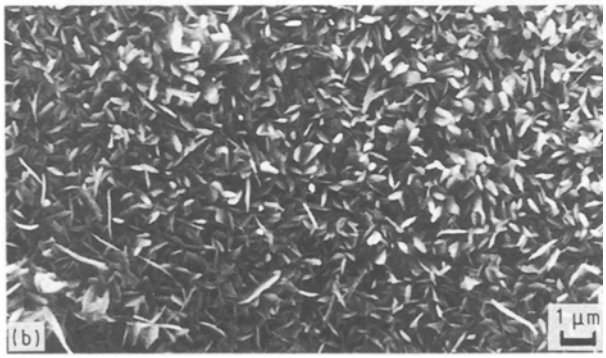

Figure 9 Oxide morphology of samples oxidized for 25 h at (a) 1000 °C, (b) 1050 °C and (c) 1100 °C.

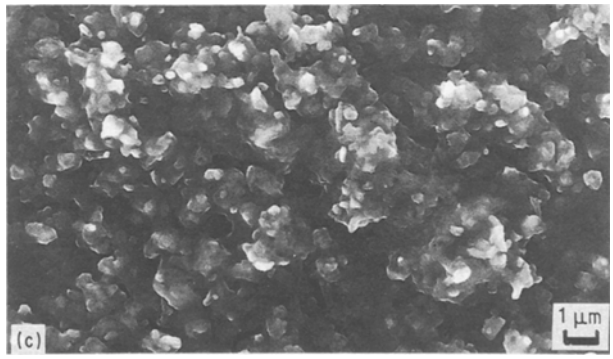

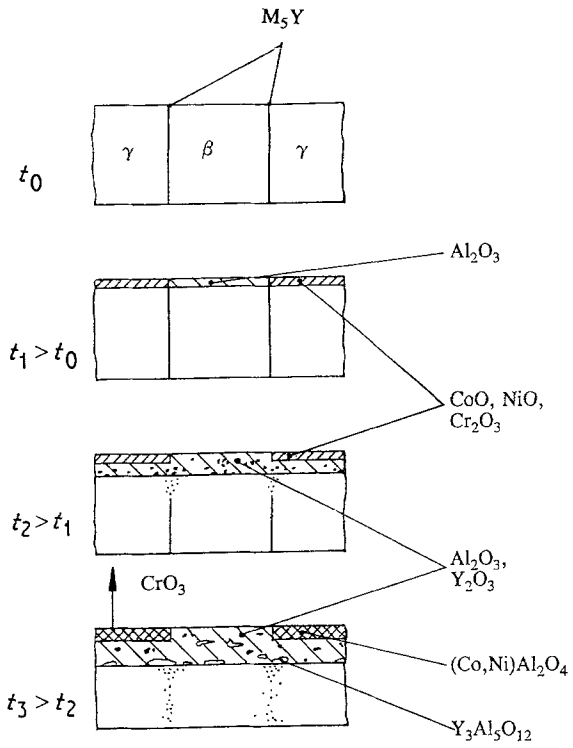

Figure 10 Model of the oxidation mechanism at 1100 °C.

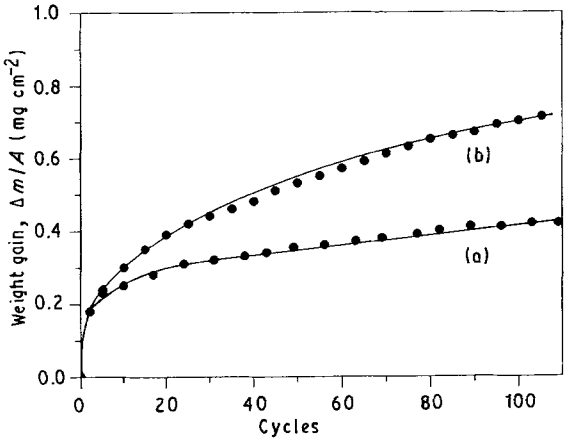

Figure 11 Cyclic oxidation at (a) 1000 and (b) 1100 °C.

bound as intermetallic M_5Y and did not influence the oxidation process.

2. The temperature range between 1000 and 1100 °C was characterized by the beginning of dissolution of the intermetallic M_5Y phases. A transition from chromia- to alumina-determined oxide growth was observed. This fact explained the parabolic rate constants k_p which were independent of the oxidation temperature. In this temperature range the oxide morphology changed significantly from a loose to a compact structure.

3. Above 1100 °C the yttrium became entirely effective. The oxidation rate was determined by the growth of alumina. Since all Y_2O_3 changed to YAG, the spalling of the oxide occurred at temperatures above 1200 °C.

4. Cyclic oxidation measurements prove the NiCoCrAlY coating material to be resistant to thermal shock. For temperatures of 1000 and 1100 °C no differences between isothermal and cyclic oxidation were found with respect to their oxidation rates.

Acknowledgements

The authors express their appreciation to Ms H. Malks and Mr A. Kehrel for technical assistance. Thanks are also due to H. C. Starck Inc. for supplying Amperit 410 and to the Deutsche Forschungsgemeinschaft for financial aid within the Sfb 339 "Schaufeln und Scheiben in Gasturbinen–Werkstoff-und Bauteilverhalten".

References

1. F. H. STOTT, *Rep. Prog. Phys.* **50** (1987) 861.
2. G. W. GOWARD, *Mater. Sci. Technol.* **2** (1986) 194.
3. V. THIEN, F. SCHMITZ, W. SLOTTY and W. VOSS, *Fresenius Z. Anal. Chem.* **319** (1984) 646.
4. R. BÜRGEL, H. W. GRÜNLING and K. SCHNEIDER, *Werkstoffe Korros.* **38** (1987) 549.
5. A. KUMAR, M. NASRALLAH and D. L. DOUGLAS, *Oxidation Met.* **8** (1974) 227.
6. J. F. COLLINS, V. P. CALKINS and J. A. McGARTY, in "The Rare Earths and Related Metals" (American Society for Metals, Metals Park, Ohio, 1960) p. 499.
7. A. M. KUNTZ, *Mater. Sci. Engng* **87** (1987) 251.
8. ST MROWEC, A. GIL and A. JEDLINSKI, *Werkstoffe Korros.* (1987) 563.
9. H. -D. STEFFENS, in "Coatings for High Temperature Applications", edited by E. Lang (Applied Science Publishers, London, 1983) p. 121.
10. R. BÜRGEL, *VDI-Berichte* **624** (1986) 185.
11. A. M. HUNTZ, *Mater. Sci. Forum* **43** (1989) 131.
12. K. P. LILLERUD and P. KOFSTAD, *J. Electrochem. Soc.* **127** (1980) 2397.
13. H. HINDAM and D. P. WHITTLE, *Oxidation Met.* **18** (1983) 245.
14. C. D. WAGNER, W. M. RIGGS, L. E. DAVIS and J. F. MOULDER, in "Handbook of X-ray Photoelectron Spectroscopy", edited by G. E. Muilenberg (Perkin–Elmer Corporation, Eden Prairie, Minnesota, 1979) 27.
15. S. SACRE, U. WIENSTROTH, H. -G. FELLER and L. K. THOMAS, *Mater. Sci. Engng* **A145** (1991) L23.
16. K. PRZYBYLSKI and G. J. YUREK, *Mater. Sci. Forum* **43** (1989) 1.
17. I. M. ALLAM, D. P. WHITTLE and J. STRINGER, *Oxidation Met.* **12** (1978) 35.

Received 12 December 1991
and accepted 2 September 1992